A New Iterative Estimation Procedure for the Localization of Passive Stationary Objects from Received RF Signals in Indoor Environments

Rym Hicheri
Faculty of Engineering and Science
University of Agder
NO-4898 Grimstad, Norway
rym.hicheri@uia.no

Matthias Pätzold
Faculty of Engineering and Science
University of Agder
NO-4898 Grimstad, Norway
matthias.paetzold@uia.no

***Abstract*—This paper deals with the localization of passive stationary objects from the received radio-frequency (RF) signals in 3-dimensional (3D) indoor environments. Each object located in the 3D indoor environment is modelled by a single point scatterer. The propagation space is equipped with a multiple-input multiple-output (MIMO) wireless communication system. The employed channel model is flexible and allows to have a line-of-sight (LOS) component as well as single- and double-bounce scattering components. Here, we present a new accurate iterative estimation technique for computing the optimal coordinates as well as the number of the main stationary objects (scatterers) in indoor areas. The proposed approach aims at matching the frequency correlation function (FCF) of the transfer function (TF) of the received RF signals to the FCF of the channel model. This iterative procedure is based on numerical optimization techniques to estimate the number and coordinates of the scatterers and the channel parameters by minimizing the Euclidean norm of the fitting error. Numerical results are presented to confirm the accuracy of the proposed estimation procedure by comparing the estimated positions as well as the resulting FCF with the corresponding exact quantities, known from generated RF signals.**

***Index Terms*—Object localization, iterative estimation technique, stationary channels, indoor environments, RF signals, multiple-input multiple-output systems.**

I. Introduction

In recent years, precise object localization has attracted much attention due to its wide range of applications [1]–[4]. In the case of outdoor localization, several popular and successful positioning systems have been developed, e.g., global positioning system (GPS), Galileo, Glonass, and BeiDou [5]. Since indoor channels are subject to attenuation, rich scattering, and multipath propagation, these technologies cannot be applied to indoor areas. Therefore, there has been great interest in investigating wireless indoor localization techniques [1], [4], [6], [7].

Indoor localization approaches can be classified according to the techniques they employ: ultra-wideband (UWB), infra-red, ultra-sound, Wi-Fi, wireless sensor networks, and vision (image) processing [4], [7]. For the special case of Wi-Fi technology, and due to their widespread indoor deployment, several Wi-Fi-based localization methods have been proposed. Among these methods, one can find the propagation model (PM)-based approaches, the time of arrival (TOA)-based methods, the time difference of arrival (TDOA)-based techniques, the angle of arrival (AOA)-based methods, and the fingerprinting-based algorithms [4], [7]–[11]. With the increasing presence of cameras (both single cameras as well as camera networks) in people's everyday lives, heterogeneous designs of radio-frequency (RF) positioning techniques with image processing were also reported, e.g., [12]. From the aforementioned references, it can be concluded that the existing RF-based positioning methods have two major disadvantages. First, these techniques are technology-dependent, which means that the localization method must be adapted to the requirements of the considered technology. Secondly, their performance is strongly influenced by the presence of the line-of-sight (LOS) component and the rich scattering conditions resulting from stationary objects such as walls, floors, decoration objects, and furniture. The purpose of this paper is to contribute to the topic of the localization of passive stationary objects in indoor environments while taking into account the LOS, single-bounce scattering, and double-bounce scattering components.

Several iterative channel estimation techniques have been reported [13]–[17] for the parametrization of channel models. The estimation of signal parameters via rotational invariance techniques (ESPRIT) is a very popular AOA estimation method [16], [17]. Maximum-likelihood-based algorithms, such as the expectation maximization [15] and the space alternating generalized expectation maximization (SAGE) [18], [19] algorithms have also been proven to be reliable estimation technique to compute the parameters of measurement-based channel simulation models. Later, the iterative non-linear least square approximation (INLSA) algorithm was introduced in the context of the design of measurement-based wideband channel simulators [20], [21]. As can be seen from [21] and [22], the INLSA algorithm has been applied to both the time-frequency correlation function and time-variant impulse response to simultaneously determine the path gains, Doppler frequencies, and path delays. Unfortunately, the output quantities of the aforementioned methods do not provide any information on the positions of the scatterers.

To fill the gaps of the aforementioned techniques, we fur-

ther extend the INLSA method to estimate the positions of passive stationary objects which are modelled by stationary point scatterers from the received RF signals in 3D indoor environments. To do so, we start by introducing a new 3D multiple-input multiple-output (MIMO) channel simulation model that includes the presence of LOS components and considers both single-bounce and double-bounce scattering components. Then, the proposed iterative approach aims at matching the frequency correlation function (FCF) of the transfer function (TF) of the received RF signals as close as possible to the FCF of the channel simulation model. The positions of the scatterers are obtained through numerical optimization by minimizing the Euclidean norm of the fitting error. We take into account that the path gains and path delays depend on the coordinates of the scatterers. In addition, this positioning algorithm allows a more accurate knowledge of indoor environments by providing information on the number and positions of the main stationary objects contributing to the multipath propagation phenomenon. The accuracy of the proposed estimation technique has been verified by comparing the obtained estimated parameters of interest, i.e., positions of the stationary scatterers, with those of the known RF test signals generated by means of computer simulations.

The remainder of this paper is organized as follows. Section II describes the indoor scenarios investigated. In Section III, we introduce the 3D channel model and its key features. The proposed iterative estimation method is the subject of Section III. Section IV presents some numerical examples and results. Finally, the conclusion is drawn in Section V.

II. Scenario Description

In this section, we describe the investigated indoor propagation scenario. As shown in Fig. 1, we consider a typical example of a room with length A, width B, and height H. The indoor space is equipped with a MIMO communication system. The transmitter T_X and the receiver R_X are equipped with uniform linear antenna arrays consisting of N_T and N_R equi-spaced antenna elements A_j^T and A_i^R ($j = 1, 2, \ldots, N_T$ and $i = 1, 2, \ldots, N_R$), respectively. There are several passive stationary objects in the indoor area, such as walls, furniture, and decoration items.

For simplicity, the propagation phenomenon taking place in the indoor environments is modelled by means of the 3D geometrical channel model depicted in Fig. 2. As can be seen from Fig. 2, the centre O_T of the transmitter T_X is assumed to be located at the centre of the reference mark, which may differ from the centre O of the room. The centre O_R of the receiver R_X is located at the coordinates (x_0^R, y_0^R, z_0^R). The distance D_0 between O_T and O_R is $D_0 = [(x_0^R)^2 + (y_0^R)^2 + (z_0^R)^2]^{1/2}$. The antenna element spacing of the T_X and the R_X are denoted by δ_T and δ_R, respectively. The parameters α_z^T (α_z^R) and α_{xy}^T (α_{xy}^T) refer to the vertical and horizontal tilt angles of the transmitter T_X

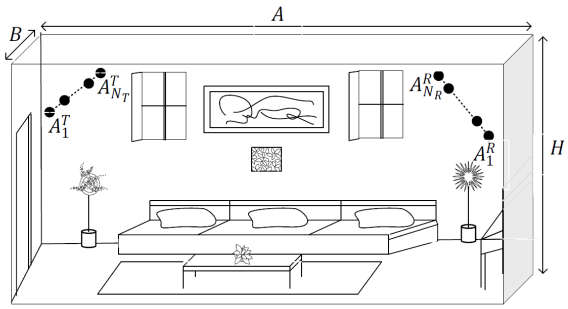

Fig. 1. A typical room architecture with the MIMO communication system and the stationary objects, such as walls, furniture etc.

(receiver R_X), respectively. The coordinates (x_j^T, y_j^T, z_j^T) of the jth transmit antenna A_j^T are given by

$$x_j^T = \left[\frac{(N_T-1)\,\delta_T}{2} - (j-1)\delta_T\right]\sin\left(\alpha_z^T\right)\cos\left(\alpha_{xy}^T\right) \quad (1)$$

$$y_j^T = -\left[\frac{(N_T-1)\,\delta_T}{2} - (j-1)\delta_T\right]\sin\left(\alpha_z^T\right)\sin\left(\alpha_{xy}^T\right) \quad (2)$$

and

$$z_j^T = \left[\frac{(N_T-1)\,\delta_T}{2} - (j-1)\delta_T\right]\cos\left(\alpha_z^T\right) \quad (3)$$

respectively. The ith receive antenna A_i^R is located at the position (x_i^R, y_i^R, z_i^R), where

$$x_i^R = x_0^R + \left[\frac{(N_R-1)\,\delta_R}{2} - (i-1)\delta_R\right]\sin\left(\alpha_z^R\right)\cos\left(\alpha_{xy}^R\right) \quad (4)$$

$$y_i^R = y_0^R - \left[\frac{(N_R-1)\,\delta_R}{2} - (i-1)\delta_R\right]\sin\left(\alpha_z^R\right)\sin\left(\alpha_{xy}^R\right) \quad (5)$$

and

$$z_i^R = z_0^R + \left[\frac{(N_R-1)\,\delta_R}{2} - (i-1)\delta_R\right]\cos\left(\alpha_z^R\right). \quad (6)$$

These objects are modelled by N scatterers S_n, $n = 1, 2, \ldots, N$, which are represented by the symbol ($\bullet$) and are located at the positions (x_n, y_n, z_n), $n = 1, 2, \ldots, N$. As illustrated in Fig. 2, the quantity D_{jn}^T (D_{in}^R), $j = 1, 2, \ldots, N_T$ ($i = 1, 2, \ldots, N_R$), represents the distance between the jth (ith) transmit (receive) antenna element A_j^T (A_i^R) and the nth stationary scatterer S_n for $n = 1, 2, \ldots, N$. Also, the symbol D_{nk} refers to distance between the fixed scatterers S_n and S_k, for $n, k = 1, 2, \ldots, N$ and $n \neq k$. In the following, we will consider single- and double-bounce scattering as well as the presence of LOS components when modelling the 3D stationary channel.

III. The Channel Model

In this section, we describe the analytical 3D stationary channel model that will later be used to estimate the position of the fixed scatterers in indoor areas. We consider an indoor environment equipped with an $N_T \times N_R$ MIMO communication system. It is assumed that the transmitted signals travels along a finite number of paths before reaching the

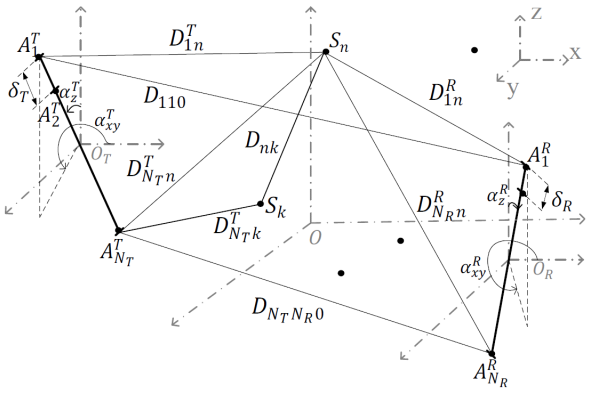

Fig. 2. The 3D geometrical model for an $N_T \times N_R$ MIMO channel with fixed scatterers.

receive antennas. Based on this assumption and according to Fig.2, the TF $H_{ij}(f')$ of the multipath fading channel between the jth transmit antenna and ith receive antenna can be split into three parts. The first part $H_{ij}^{\mathrm{LOS}}(f')$ refers to the LOS component, while the second part $H_{ij}^{\mathrm{SB}}(f')$ describes the components resulting from single-bounce scattering, and the third part $H_{ij}^{\mathrm{DB}}(f')$ comprises the components resulting from double-bounce scattering. Thus, the TF $H_{ij}(f')$ can be written as

$$H_{ij}(f') = H_{ij}^{\mathrm{LOS}}(f') + H_{ij}^{\mathrm{SB}}(f') + H_{ij}^{\mathrm{DB}}(f'). \tag{7}$$

The LOS part $H_{ij}^{\mathrm{LOS}}(f')$ of the TF is expressed as

$$H_{ij}^{\mathrm{LOS}}(f') = c_{ij0} \exp\left(-j\left(\theta_{ij0} + 2\pi f' \tau'_{ij0}\right)\right) \tag{8}$$

where the path gain $c_{ij0} = C\alpha_{ij0} D_{ij0}^{-\gamma}$ and the path delay $\tau'_{ij0} = D_{ij0}/c_0$, in which C is a constant, which depends on the transmit/receive antenna gain, the transmission power as well as the wavelength [14], [23], γ is the exponent path loss dependent on the propagation environment, and c_0 is the speed of light. The parameter α_{ij0} is a binary variable that reflects the presence (equal to 1) or absence (equal to 0) of the LOS component between the jth transmit antenna A_j^T and ith receive antenna A_i^R. The symbol θ_{ij0} refers to the phase shift of the LOS component. Here, the quantity D_{ij0} represents the distance between A_j^T and A_i^R, which can be expressed as (see Fig. 2)

$$D_{ij0} = \left[\left(x_i^R - x_j^T\right)^2 + \left(y_i^R - y_j^T\right)^2 + \left(z_i^R - z_j^T\right)^2\right]^{1/2}. \tag{9}$$

The second part $H_{ij}^{\mathrm{SB}}(f')$ is given by the expression

$$H_{ij}^{\mathrm{SB}}(f') = \sum_{n=1}^{N} c_{ijn} \exp\left(-j\left(\theta_{ijn} + 2\pi f' \tau'_{ijn}\right)\right) \tag{10}$$

in which the path gain c_{ijn} and path delay τ'_{ijn} of the nth stationary scatterer S_n are determined by $c_{ijn} = C\alpha_{ijn} D_{ijn}^{-\gamma}$ and $\tau'_{ijn} = D_{ijn}/c_0$ $(n = 1, 2, \ldots, N)$, respectively. The distance D_{ijn} $(n = 1, 2, \ldots, N)$ is the total travelling distance between the jth transmit antenna and ith receive antenna via the scatterer S_n, which is given by (see Fig. 2)

$$\begin{aligned} D_{ijn} = &\left[\left(x_n - x_j^T\right)^2 + \left(y_n - y_j^T\right)^2 + \left(z_n - z_j^T\right)^2\right]^{1/2} \\ &+ \left[\left(x_i^R - x_n\right)^2 + \left(y_i^R - y_n\right)^2 + \left(z_i^R - z_n\right)^2\right]^{1/2}. \end{aligned} \tag{11}$$

Finally, the third part $H_{ij}^{\mathrm{DB}}(f')$ of the TF $H_{ij}(f')$ is expressed as

$$H_{ij}^{\mathrm{DB}}(f') = \sum_{n=1}^{N} \sum_{\substack{k=1 \\ k \neq n}}^{N} c_{ijnk} \exp\left(-j\left(\theta_{ijnk} + 2\pi f' \tau'_{ijnk}\right)\right) \tag{12}$$

where θ_{ijnk} is the phase shift. Here, the path gain c_{ijnk} and path delay τ'_{ijnk} are expressed in terms of the distance D_{ijnk} as $c_{ijnk} = \alpha_{ijnk} C D_{ijnk}^{-\gamma}$ and $\tau'_{ijnk} = D_{ijnk}/c_0$, respectively. The distance D_{ijnk} is given by the sum of the distances D_{in}^R, D_{nk}, and D_{jn}^T (see Fig. 2), i.e.,

$$\begin{aligned} D_{ijnk} = &\left[\left(x_n - x_j^T\right)^2 + \left(y_n - y_j^T\right)^2 + \left(z_n - z_j^T\right)^2\right]^{1/2} \\ &+ \left[\left(x_n - x_k\right)^2 + \left(y_n - y_k\right)^2 + \left(z_n - z_k\right)^2\right]^{1/2} \\ &+ \left[\left(x_i^R - x_n\right)^2 + \left(y_i^R - y_n\right)^2 + \left(z_i^R - z_n\right)^2\right]^{1/2}. \end{aligned} \tag{13}$$

The parameter α_{ijnk} is a binary constant that describes the presence (equal to 1) or absence (equal to 0) of the double-bounce component resulting from the bouncing effect on the scatterers S_n and S_k. In (8), (10), and (12), the phase shifts θ_{ij0}, θ_{ijn}, and θ_{ijnk} $(n, k = 1, 2, \ldots, N)$ are modelled by independent random variables, which are uniformly distributed over the interval $[0, 2\pi)$.

In this work, we consider stationary channels, for which the positions of the scatterers are fixed and thus, all channel parameters in (7) are time-independent. Then the FCF $R_{ij}(\nu') = E\{H_{ij}(f') H_{ij}^*(f' + \nu')\}$ of the TF $H_{ij}(f')$ can be expressed as follows

$$\begin{aligned} R_{ij}(\nu') = &c_{ij0}^2 \exp\left(-j2\pi\nu' \tau'_{ij0}\right) + \sum_{n=1}^{N} c_{ijn}^2 \exp\left(-j2\pi\nu' \tau'_{ijn}\right) \\ &+ \sum_{n=1}^{N} \sum_{\substack{k=1 \\ k \neq n}}^{N} c_{ijnk}^2 \exp\left(-j2\pi\nu' \tau'_{ijnk}\right) \end{aligned} \tag{14}$$

where $E\{\cdot\}$ is the statistical averaging operator and $(\cdot)^*$ denotes complex conjugation.

The main purpose of this paper is to propose a new iterative procedure to estimate the positions of fixed objects (scatterers) by utilizing the TF in (14). The formulation of this estimation technique will be the subject of the next section. In the following, we assume that all parameters (positions and tilt angles) related to the transmitter T_X and the receiver R_X are known.

IV. The Estimation Algorithm

In reality, the TF $\hat{H}(f'_q)$ of the measured channel is computed from a snapshot of the received RF signal at discrete frequency instances $f'_q = -B/2 + q\Delta f' \in [-B/2, B/2]$,

$q = 1, 2, \ldots, Q$, with B being the measured frequency bandwidth. The frequency interval $\Delta f'$ is a known characteristic of the channel sounder employed to collect the measurement data. Consequently, the FCF of the measured discrete TF can be represented in the form of a discrete function $\hat{R}_{ij}(\nu'_q)$ ($j = 1, 2, \ldots, N_T$ and $i = 1, 2, \ldots, N_R$). Accordingly, the TF $H(f')$ of the channel model given in (7) and, thus, the corresponding FCF $R_{ij}(\nu'_q)$ can be derived from (14) by replacing ν' by ν'_q.

Here, the problem is to determine the positions (x_n, y_n, z_n) of the scatterers S_n, $n = 1, 2, \ldots, N$. To do so, we must determine a set of parameters $\mathcal{P} = \{C, x_n, y_n, z_n, n = 1, 2, \ldots, N\}$ by fitting the FCF $R_{ij}(\nu'_q)$ of the 3D indoor channel model as close as possible to the FCF $\hat{R}_{ij}(\nu'_q)$ of the measured channel, i.e.,

$$\mathcal{P} = \underset{\mathcal{P}}{\operatorname{argmin}} \sum_{j=1}^{N_T} \sum_{i=1}^{N_R} \left\| \hat{R}_{ij}(\nu'_q) - R_{ij}(\nu'_q) \right\|_2^2 \tag{15}$$

where $||\cdot||$ denotes the Euclidean norm. To compute the coordinates of the scatterers S_n, we introduce the objective function $E(\mathcal{P})$ as

$$E(\mathcal{P}) = \sum_{j=1}^{N_T} \sum_{i=1}^{N_R} \left\| \hat{R}_{ij}(\nu'_q) - R_{ij}(\nu'_q) \right\|_2^2. \tag{16}$$

The purpose is to estimate the positions and the number of scatterers in the propagation space by minimizing the objective function in (16). To do so, we start by setting $n_0 = N = 1$, and for arbitrary chosen values of $C^{(0)}$, $x_{n_0}^{(0)}$, $y_{n_0}^{(0)}$, and $z_{n_0}^{(0)}$, we introduce the error function for the n_0th scatterer at every iteration l ($l = 0, 1, 2, \ldots$) as

$$y_{ijn_0}^{(l)}(\nu'_q) = \hat{R}_{ij}(\nu'_q) - \sum_{\substack{n=1 \\ n \neq n_0}}^{N} \left(c_{ijn}^{(l)}\right)^2 \exp\left(-j2\pi\nu'_q \left(\tau'_{ijn}\right)^{(l)}\right) - \sum_{\substack{n=1 \\ n \neq n_0}}^{N} \sum_{\substack{k=1 \\ k \neq n}}^{N} \left(c_{ijnk}^{(l)}\right)^2 \exp\left(-j2\pi\nu'_q \left(\tau'_{ijnk}\right)^{(l)}\right). \tag{17}$$

The new estimates of $C^{(l+1)}$, $x_{n_0}^{(l+1)}$, $y_{n_0}^{(l+1)}$, and $z_{n_0}^{(l+1)}$ corresponding to the n_0th scatterer (propagation path) S_{n_0} are obtained from the error function $y_{ijn_0}^{(l)}(\nu'_q)$ in (17) as

$$\left(C^{(l+1)}, x_{n_0}^{(l+1)}, y_{n_0}^{(l+1)}, z_{n_0}^{(l+1)}\right) = \underset{\mathcal{P}}{\operatorname{argmin}} \sum_{j=1}^{N_T} \sum_{i=1}^{N_R} \left\| \mathbf{y}_{ijn_0}^{(l)} - c_{ij0}^2 \exp\left(-j2\pi\nu'_q \tau'_{ij0}\right) - c_{ijn_0}^2 \exp\left(-j2\pi\nu'_q \tau'_{ijn_0}\right) \right\|_2^2 \tag{18}$$

where $\mathbf{y}_{ijn_0}^{(l)}$ is a column vector containing the stacked values of $y_{ijn_0}^{(l)}(\nu'_q)$ for increasing values of q. Note that the value of the parameter α_{ij0} is chosen to minimize the relative error in the objective function in (17).

Now, let us assume fixed values of $x_{n_0}^{(l)}$, $y_{n_0}^{(l)}$, and $z_{n_0}^{(l)}$. Inserting $c_{ijn} = C D_{ijn}^{-\gamma}$ in (18) and then, deriving the right-hand side of (18) with respect to the variable C yields the following exact closed-form expression for the new estimate of $C^{(l)}$

$$C^{(l+1)} = \left[\sum_{j=1}^{N_T} \sum_{i=1}^{N_R} \left(\mathbf{s}_{ijn_0}^{(l)}\right)^H \mathbf{s}_{ijn_0}^{(l)} \right]^{-\frac{1}{2}} \left[\sum_{j=1}^{N_T} \sum_{i=1}^{N_R} \left[\operatorname{Re}\left\{\mathbf{y}_{ijn_0}^{(l)}\right\}^T \cdot \operatorname{Re}\left\{\mathbf{s}_{ijn_0}^{(l)}\right\} + \operatorname{Im}\left\{\mathbf{y}_{ijn_0}^{(l)}\right\}^T \operatorname{Im}\left\{\mathbf{s}_{ijn_0}^{(l)}\right\} \right] \right]^{\frac{1}{2}} \tag{19}$$

where $(\cdot)^T$ and $(\cdot)^H$ are the transpose and Hermitian operators, respectively. The symbol $\mathbf{s}_{ijn_0}^{(l)}$ refers to the column vector containing the stacked values of the function $D_{ij0}^{-2\gamma} \exp(-j2\pi\nu'_q \tau'_{ij0}) + D_{ijn_0}^{-2\gamma} \exp(-j2\pi\nu'_q \tau'_{ijn_0})$ for increasing values of q. The operators $\operatorname{Re}\{\cdot\}$ and $\operatorname{Im}\{\cdot\}$ denote the real part and imaginary part, respectively.

By substituting (19) in (18), the optimization problem in (18) reduces to

$$\left(x_{n_0}^{(l+1)}, y_{n_0}^{(l+1)}, z_{n_0}^{(l+1)}\right) = \underset{\mathcal{P}\setminus\{C\}}{\operatorname{argmin}} \sum_{j=1}^{N_T} \sum_{i=1}^{N_R} \left\| \mathbf{y}_{ijn_0}^{(l)} - \left(C^{(l+1)}\right)^2 \cdot \left[D_{ij0}^{-2\gamma} \exp\left(-j2\pi\nu'_q \tau'_{ij0}\right) - D_{ijn_0}^{-2\gamma} \exp\left(-j2\pi\nu'_q \tau'_{ijn_0}\right) \right] \right\|_2^2. \tag{20}$$

Then, the new estimates of the coordinates $x_{n_0}^{(l+1)}$, $y_{n_0}^{(l+1)}$, and $z_{n_0}^{(l+1)}$ of the position of the n_0th scatterer S_{n_0} are numerically computed by minimizing the right-hand side of (20). The iterative steps given in (17)−(20) proceed as long as the relative change in the objective function $E(\mathcal{P})$ in (16) is larger than or equal to a predetermined error level ε_1. When the relative change in $E(\mathcal{P})$ becomes smaller than the error level ε_1, the number of scatterers N is increased by 1, i.e., $N \longleftarrow N + 1$. Then, for arbitrarily chosen initial values of $C^{(0)}$, $x_N^{(0)}$, $y_N^{(0)}$, and $z_N^{(0)}$, using the error function

$$y_{ijN}^{(l)}(\nu'_q) = \hat{R}_{ij}(\nu'_q) - \sum_{n=1}^{N-1} \left(c_{ijn}^{(l)}\right)^2 \exp\left(-j2\pi\nu'_q \left(\tau'_{ijn}\right)^{(l)}\right) - \sum_{n=1}^{N-1} \sum_{\substack{k=1 \\ k \neq n}}^{N-1} \left(c_{ijnk}^{(l)}\right)^2 \exp\left(-j2\pi\nu'_q \left(\tau'_{ijnk}\right)^{(l)}\right) \tag{21}$$

allows us to compute the new estimates of the parameters $C^{(l+1)}$, $x_N^{(l+1)}$, $y_N^{(l+1)}$, and $z_N^{(0l+1)}$ by following the steps presented in (18)−(20) for $n_0 = N$. Here again, the value of the binary parameter α_{ijn_0k} is chosen to minimize the relative error in the objective function $E(\mathcal{P})$ in (16). The estimation method is then repeated until no further progress can be made by increasing the value of N or a predetermined maximum number of propagation paths $N_{\max}$ is reached. Thus, the output of the proposed algorithm is an estimate of the number and the positions of the main fixed scatterers contributing to the multipath propagation phenomenon in the considered stationary indoor environment.

V. Numerical Results

In this section numerical results are presented to validate the accuracy and applicability of the proposed iterative procedure for estimating the positions of stationary objects in

propagation environments modelled here by fixed scatterers. To do so, one compares the exact locations of the scatterers with those obtained by applying the proposed localization technique.

For the performance analysis, we consider a room with length $A = 10\,\text{m}$, width $B = 5\,\text{m}$, and height $H = 2.5\,\text{m}$. We assume that the passive stationary objects in the indoor area are modelled by $N = 10$ fixed scatterers obtained from the outcomes of a random generator with uniform distribution inside the room. The centres O_T and O_R of the transmitter T_X and the receiver R_X are located, with respect to the centre of the room O, at the positions $(-4.5, 0, 1)$ and $(3, 1, -0.5)$, respectively. As it is assumed that the centre O_T is the centre of the reference, the centre of the receiver R_X is located at the position $(7.5, 1, 1.5)$ with respect to the reference of centre O_T (see Fig. 2). The number of transmit antennas and receive antennas are set to $N_T = N_R = 8$. The antennas spacings δ_T and δ_R are equal to 0.1 m. The antennas are located along the y axis, i.e., $\alpha_z^T = \alpha_z^R = -\pi/2$ and $\alpha_{xy}^T = \alpha_{xy}^R = \pi/2$. The predefined error level ε is set to 0.01. A summary of the simulation parameters can be found in Table I.

For the numerical results presented in Fig. 3, the coordinates x_n, y_n, and z_n of the nth scatterer S_n $(n = 1, 2, \ldots, N)$ are chosen randomly. Let X_n, Y_n, and Z_n be random variables which are uniformly distributed over the intervals [-5,5], [-2.5,2.5], and [-1.25,1.25], respectively. Then, the quantities x_n, y_n, and z_n correspond to a realisation of the random variables X_n, Y_n, and Z_n, respectively. We assume there are two multipath components resulting from double-bounce scattering, in which the scatterers S_1, S_3, S_4, and S_5 are involved. In Fig. 3, we present the indoor area considered for the validation of the proposed localization algorithm together with the exact positions of the stationary scatterers S_n as well as the estimated position of the scatterers S_n, $n = 1, 2, \ldots, N$. Our numerical results have shown that the presented iterative procedure results in an efficient and accurate estimation of the position of the scatterers, with an accuracy better than 15 cm and an average (over all scatterers) error of approximately 12.5 cm.

Now, we investigate the effect of the number of fixed objects (scatterers) in the room on the accuracy of the proposed positioning algorithm. For this purpose, we present in Table II the mean error (in cm) of the Euclidean distance between the exact position of the scatterers and the corresponding estimates for different values of N, namely $N = 5$, 10, 15, and 20. For each value of N, the presented quantities are computed by averaging over the scatterers and 10 scenarios, where for each scenario, the positions of the scatterers have been randomly generated. As can be seen from Table II, the average error increases with increasing values of N. For all trials, simulations have shown that the proposed algorithm estimates the correct number of fixed scatterers with an accuracy of approximately 92%.

Comparison with existing techniques: For comparison purposes, it is of interest to compare the estimation results of the proposed algorithm with those obtained by applying other RF-based positioning methods. In fact, this task is difficult to perform because the techniques developed in the context of indoor localization of stationary objects, such as in [4], [7]–[11], assume one or two objects moving at constant speed. In addition, their performance is strongly affected by fixed objects (scatterers) in the room. This is in contrast with our proposed estimation method which aims to investigate the contributions of the fixed objects in indoor spaces. Furthermore, channel parameter estimators reported

TABLE I
SIMULATION PARAMETERS

Symbol	Name	Value
A	Room length	10 m
B	Room width	5 m
H	Room height	2.5 m
N_T	Number of transmit antennas	8
N_R	Number of receive antennas	8
δ_T	Transmit antennas spacing	0.1 m
δ_R	Receive antennas spacing	0.1 m
α_z^T	Vertical tilt angle of the T_X	-$\pi/2$
α_{xy}^T	Horizontal tilt angle of the T_X	$\pi/2$
α_z^R	Vertical tilt angle of the R_X	-$\pi/2$
α_{xy}^R	Horizontal tilt angle of the R_X	$\pi/2$
N	Number of stationary objects	10
C	Hardware dependent parameter	1.5
γ	Propagation environment parameter	2
ε	Predefined error level	0.01

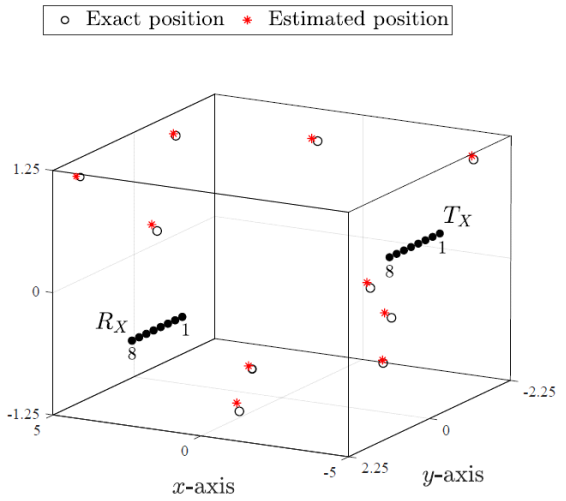

Fig. 3. Estimation results with $N = 10$ and $N_T = N_R = 8$.

TABLE II
EFFECT OF THE NUMBER OF FIXED OBJECTS ON THE PERFORMANCE OF THE ESTIMATION METHOD

Number of objects N	5	10	15	20
Average error (in cm)	12.01	13.26	16.24	20.72

in the context of mobile radio communications, such as the INLSA algorithm [21], [22], cannot be employed. This is because they assume a mobile transmitter/receiver as well as a simpler channel model (without taking into account the effect of the distance travelled on the channel parameters) and return a set of parameters from which the optimal coordinates of the scatterers cannot be retrieved. Hence, a fair comparison with other estimation techniques cannot be presented.

VI. Conclusion

This paper contributes to the localization of passive stationary objects in 3D indoor environments by proposing a new, accurate, and reliable positioning algorithm, where the indoor area is equipped with a MIMO communication system. First, we have introduced a generic 3D stationary channel model that offers the flexibility to have LOS components and both single- and double-bounce scattering components. The proposed algorithm estimates the positions of the fixed scatterers by fitting the FCF of the TF of the received RF signals as closely as possible to the FCF of the multipath channel model. The coordinates of the stationary objects are computed by minimizing the Euclidean norm of the error function. Together with the fixed scatters' positions, this estimation technique allows the determination of the path gains and path delays, i.e., the parametrization of the channel model. In addition, it provides information on the positions as well as the number of the passive stationary objects in the considered indoor space, which in turn allows a better understanding of the resulting multipath propagation phenomenon (rich scattering). The accuracy and validity of the proposed iterative estimation procedure have been confirmed by comparing the positions of the scatterers with their exact positions, known from test RF signals generated by indoor channel simulations. Future work will focus on the extension of this algorithm to the localization of active moving objects or persons in indoor environments with strong stationary scattering components.

Acknowledgement

This work was supported by the WiCare Project funded by the Research Council of Norway under grant number 261895/F20.

References

[1] Y. Gu, A. Lo, and I. Niemegeers, "A survey of indoor positioning systems for wireless personal networks," *IEEE Commun. Surveys Tuts.*, vol. 11, no. 1, Mar. 2009.

[2] M. Yassin and E. Rachid, "A survey of positioning techniques and location based services in wireless networks," in *IEEE Inte. Conf. on Signal Proc., Inf., Commun. and Energy Syst. (SPICES'15)*, Kozhikode, India, Feb. 2015, pp. 1–5.

[3] Q. D. Vo and P. De, "A survey of fingerprint-based outdoor localization," *IEEE Commun. Surveys Tuts*, vol. 18, no. 1, pp. 491–506, 1st Quart., 2016.

[4] A. Yassin et al., "Recent advances in indoor localization: A survey on theoretical approaches and applications," *IEEE Commun. Surveys Tuts.*, vol. 19, no. 2, pp. 1327–1346, 2nd Quart., 2017.

[5] "The business advantages of a multi-GNSS set-up," Available: https://www.telit.com/blog/multi-gnss-business-advantages/.

[6] H. Liu, H. Darabi, P. Banerjee, and J. Liu, "Survey of wireless indoor positioning techniques and systems," *IEEE Trans. Syst., Man, and Cybern., Part C, Appl. Reviews*, vol. 37, no. 6, pp. 1067–1080, Nov. 2007.

[7] S. He and S.-H. G. Chan, "Wi-Fi fingerprint-based indoor positioning: Recent advances and comparisons," *IEEE Commun. Surveys Tuts.*, vol. 18, no. 1, pp. 466–490, 1st Quart., 2016.

[8] Y.-L. Sun and Y.-B. Xu, "Error estimation method for matrix correlation-based Wi-Fi indoor localization.," *KSII Trans. Internet Inf. Syst.*, vol. 7, no. 11, pp. 2657–2675, Nov. 2013.

[9] P. Gallo and S. Mangione, "RSS-eye: Human-assisted indoor localization without radio maps," in *IEEE Int. Conf. on Commun. (ICC'15)*, Jun. 2015, pp. 1553–1558.

[10] A. Makki, A. Siddig, M. Saad, J. R. Cavallaro, and C. J. Bleakley, "Indoor localization using 802.11 time differences of arrival," *IEEE Trans. Instrum. Meas.*, vol. 65, no. 3, pp. 614–623, London, UK, Mar. 2016.

[11] T. A. Heya, S. E. Arefin, A. Chakrabarty, and M. Alam, "Image processing based indoor localization system for assisting visually impaired people," in *Ubiquitous Positioning, Indoor Navigation and Location-Based Services (UPINLBS'18)*, Wuhan, China, Dec. 2018, pp. 1–7.

[12] T. V. Nguyen, Y. Jeong, D. P. Trinh, and H. Shin, "Location-aware visual radios," *IEEE Wireless Commun.*, vol. 21, no. 4, pp. 28–36, Aug. 2014.

[13] R. Schmidt, "Multiple emitter location and signal parameter estimation," *IEEE Trans. Antennas and Propag.*, vol. 34, no. 3, pp. 276–280, Mar. 1986.

[14] C. Phillips, D. Sicker, and D. Grunwald, "A survey of wireless path loss prediction and coverage mapping methods," *IEEE Commun. Surveys Tuts*, vol. 15, no. 1, pp. 255–270, 1st Quart., 2013.

[15] M. Feder and E. Weinstein, "Parameter estimation of superimposed signals using the EM algorithm," *IEEE Trans. Acoust. , Speech, Signal Processing*, vol. 36, no. 4, pp. 477–489, Apr. 1988.

[16] R. Roy and T. Kailath, "ESPRIT-Estimation of signal parameters via rotational invariance techniques," *IEEE Trans. Acoust. , Speech, Signal Processing*, vol. 37, no. 7, pp. 984–995, Jul. 1989.

[17] A.-J. Van Der Veen, M. C. Vanderveen, and A. Paulraj, "Joint angle and delay estimation using shift-invariance techniques," *IEEE Trans. Signal Processing*, vol. 46, no. 2, pp. 405–418, Feb. 1998.

[18] B. H. Fleury, M. Tschudin, R. Heddergott, D. Dahlhaus, and K. I. Pedersen, "Channel parameter estimation in mobile radio environments using the SAGE algorithm," *IEEE J. Select. Areas Commun.*, vol. 17, no. 3, pp. 434–450, Mar. 1999.

[19] W. Li, W. Yao, and P. J. Duffett-Smith, "Improving the SAGE algorithm with adaptive partial interference cancellation," in *IEEE 13th Digital Signal Processing Workshop and 5th IEEE Signal Processing Education Workshop (DSP/SPE'09)*, Marco Island, FL, USA, Jan. 2009, pp. 404–409.

[20] D. Umansky and M. Pätzold, "Design of measurement-based wideband mobile radio channel simulators," in *4th Int. Symp. on Wireless Commun. Systems (ISWCS'07)*, Trondheim, Norway, Oct. 2007, pp. 229–235.

[21] A. Fayziyev and M. Pätzold, "An improved iterative nonlinear least square approximation method for the design of measurement-based wideband mobile radio channel simulators," in *Int. Conf. on Advanced Technol. for Commun. (ATC'11)*, Da Nang, Vietnam, 2011, pp. 106–111.

[22] A. Fayziyev and M. Pätzold, "The performance of the INLSA in comparison with the ESPRIT and SAGE algorithms," in *Int. Conf. on Advanced Technol. for Commun. (ATC'14)*, Hanoi, Vietnam, Feb. 2014, pp. 332–337.

[23] A. Borhani and M. Pätzold, "A non-stationary channel model for the development of non-wearable radio fall detection systems," *IEEE Trans. Wireless Commun.*, vol. 17, no. 11, pp. 7718–7730, Sept. 2018.